INTERFACE SHEAR TRANSFER FOR HIGH STRENGTH CONCRETE AND HIGH STRENGTH REINFORCEMENT

Susumu KONO[1] And Hitoshi TANAKA[2]

SUMMARY

The shear transfer at construction joints for members with high strength concrete and shear friction reinforcement was studied experimentally using twenty-three direct shear type specimens. The contribution of dowel action to the total shear increased from 0% to about 60% as slip increased up to 4 mm. The larger the area and the yield strength of reinforcement, the smaller the stress drop after the initial peak and the larger the stress regain after the drop. The shear capacity also increased linearly with the normal force provided by reinforcement but it was found that reinforcing bars did not yield when the shear capacity was reached. The interface roughness was measured using laser digitizing devices and quantified with indices in order to correlate the surface roughness to stiffness and capacity in shear. Although those indices did not show the clear correlation with stiffness and capacity, the surface roughness is considered to affect the stress of reinforcement at the maximum shear, in addition to other factors like the area and yield strength of reinforcement and the concrete strength. A more appropriate index is under search to express surface roughness which can be correlated to the shear transfer mechanisms. With a linear approximation of the relation between the stress at the maximum shear and yield strength of reinforcement, an equation to evaluate the shear capacity was proposed, the format of which is similar to that of Mattock and Hawkins' [7].

INTRODUCTION

Interface shear at construction joints is transferred mainly through concrete before cracking, and through both concrete and reinforcing bars after cracking. The shear transfer through concrete is called a conrete action in this paper and consists of friction resulting from the normal compressive stress and the interlock of aggregate protrusions. The shear transfer through reinforcing bars is called a dowel action. Total shear stress transferred at cracked interfaces can be predicted by summing the stresses due to the concrete and dowel actions. The shear friction method introduced in the ACI code [1] as well as in the Japanese building code [3] is useful to account for the interface shear transfer. However, in this method, the effects of the friction at the concrete interface and the dowel action of shear-friction reinforcement are experimentally evaluated by integrating them all into the frictional coefficient, and the contribution of the dowel action to the total shear transfer cannot be directly seen from the frictional coefficient given in the codes. In addition, the contribution of the dowel action varying not only with the mechanical properties of concrete and reinforcement but also with a relative displacement between concrete surfaces is not considered, and the conventional shear friction method is not originally developed for members with high strength concrete and reinforcement. In this study, the interface shear transfer was examined experimentally using direct shear tests on 23 specimens. The concrete strength ranged from 30MPa to 100MPa and the yield strength of reinforcing bars from 350MPa to 1000MPa. The interface roughness was measured and quantified using laser digitizing devices in order to clarify its relation with stiffness and capacity in shear. The relative sliding and opening displacements and the axial force of reinforment were measured to separate the concrete and dowel actions. Based on the experimental results, a design equation for the interface shear transfer for normal and high strength materials was proposed.

[1] *Dept. of Architecuture, Kyoto University, Kyoto, Japan Email:Kono@archi.kyoto-u.ac.jp*
[2] *Dept. of Civil Eng., Toyohashi University of Technology, Toyohashi, Japan Email:Tanaka@jughead.tutrp.tut.ac.jp*

TEST SPECIMEN DESIGNS

Specimen Designs

As shown in Table 1, two series of specimens were prepared. Series 1 was designed to investigate the effects of the strength and the diameter of dowel bars, and the concrete strength on the shear transfer mechanisms, whereas Series 2 to investigate the effects of the concrete strength and the interface morphology. There were two types of specimens. C type (meaning combination) specimens had prescribed interface finishings and dowel bars embedded so that the external shear force was resisted by both concrete and dowel actions, while D type (meaning dowel) specimens were prepared to isolate the dowel action by inserting double thin plates at the interface in order to eliminate the concrete action [4]. In this manner, the external shear force was resisted by the dowel action only, in D type specimen. Specimen dimensions and reinforcement arrangement are shown in Fig. 1. For C type specimens, the lower block was cast first, a prescribed finishing made at the construction joint, and then the other half block cast. For D type specimens, lower and upper blocks were cast at a same time with double thin plates placed at the joint interface. The mechanical properties of concrete and steel are shown in Table 2. The maximum aggregate size was 20 mm.

The shear interface had four kinds of finishings as shown in Fig. 2. For a trowelled surface, laytance was removed later with a wire brush from a trowelled surface. For a rough surface, mortar on the casting surface was completely removed before concrete hardened so that a surface of an aggregate layer was seen. For a scratched surface, a grid was drawn by scratching the surface with nails before concrete hardened. For a triangle surface, a steel mold was pressed and a triangle shape was generated.

Table 1: Specimen designation and variables

Specimen			Variables			Test		
Series	Designation	Type	Type of dowel bars	Nominal f'c (MPa)	Surface Condition	τ_u (MPa)	Slip at τ_u	$\frac{\varepsilon_{cap}}{\varepsilon_y}$ *2
1	L10-30C	C	SD295A D10*1	30	Trowelled	2.98	0.56	74
	L10-30D	D			Plate	N/A	N/A	N/A
	L10-50C	C		50(A)	Trowelled	3.35	0.01	4
	L10-50D	D			Plate	N/A	N/A	N/A
	L10-80C	C		80	Trowelled	2.56	0.43	76
	L10-80D	D			Plate	N/A	N/A	N/A
	H10-30C	C	KSS785 D10*1	30	Trowelled	3.43	0.07	3
	H10-30D	D			Plate	N/A	N/A	N/A
	H10-50C	C		50(A)	Trowelled	2.95	2.00	29
	H10-50D	D			Plate	N/A	N/A	N/A
	H10-80C	C		80	Trowelled	5.16	0.61	34
	H10-80D	D			Plate	N/A	N/A	N/A
	H16-30C	C	KSS785 D16*1	30	Trowelled	4.49	2.00	28
	H16-50C	C		50(A)	Trowelled	5.83	2.00	29
	H16-80C	C		80	Trowelled	6.53	2.00	39
2	H50PC	C	KSS785 D10*1	50(B)	Trowelled	1.50	2.00	37
	H50SC	C			Scratched	2.86	2.00	61
	H50RC	C			Rough	7.31	1.45	121
	H50TC	C			Triangle	6.97	1.58	99
	H100PC	C		100	Trowelled	4.27	0.86	63
	H100SC	C			Scratched	7.11	0.95	96
	H100RC	C			Rough	8.36	2.00	80
	H100TC	C			Triangle	7.02	2.00	5

*1: D in 'D10' or 'D16' indicates a deformed bar. *2: εcap is the strain of dowel bars when the shear capacity was reached.

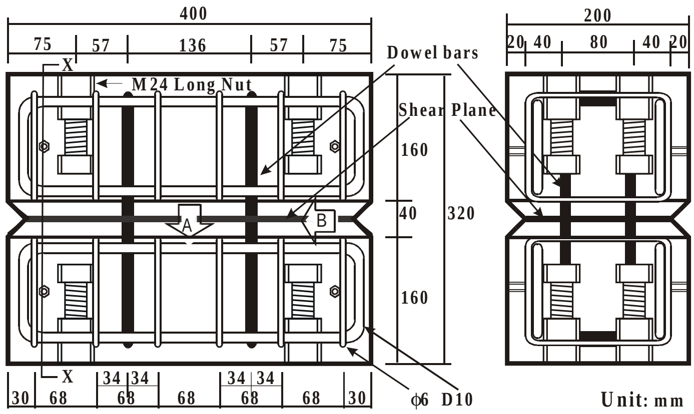

(a) Elevation (b) X-X section

Figure 1: Specimen dimensions and reinforcement arrangement

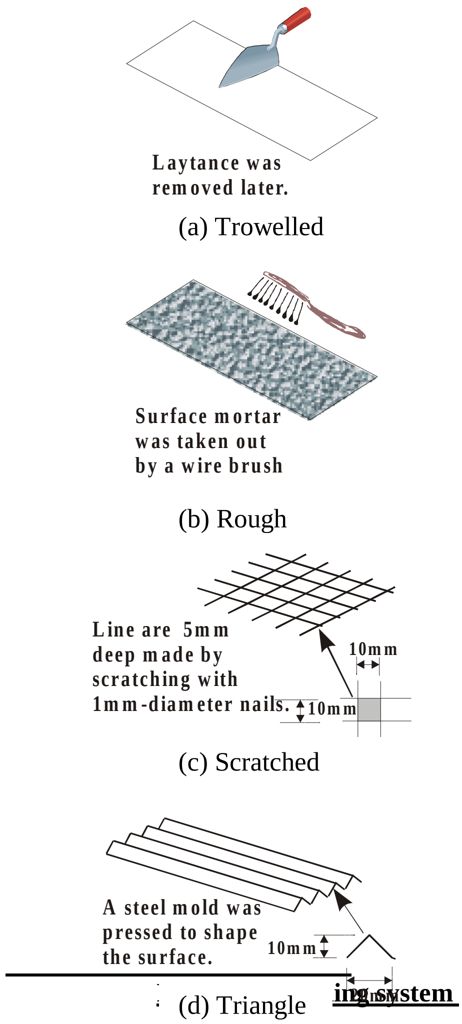

ing system

Table 2: Mechanical properties of concrete and steel

	Nominal f'c (MPa)	Block location	f'c (MPa)	f't (MPa)	Ec (GPa)
Concrete	30	Lower	30.0	3.16	25.4
		Upper	31.8	3.52	24.4
	50(A)*1	Lower	54.6	4.41	33.7
		Upper	45.4	4.44	29.2
	50(B)*1	Lower	49.0	10.7	29.2
		Upper	53.8	11.6	27.3
	80	Lower	79.2	3.31	35.6
		Upper	103	3.52	35.0
	100	Lower	103	15.7	35.4
		Upper	97.6	17.7	36.2
Steel	Bar diameter in mm^2 (Area in mm^2)	Strength Type	fy (MPa)	fu (MPa)	Es (GPa)
	10 (71.3)	SD295A	324	481	182
	10 (71.3)	KSS785	999	1034	184
	16 (198.6)		867	1085	187

*1 A and B refers to the same label for f'c=50MPa in Table 1.

Loading

Figure 3 shows the loading and measuring system. The center of the horizontal force stayed at the same height as the shear plane so that the direct shear force acted on the shear plane without moment. The vertical loading jack was used for D type specimens only. For C type specimens, the horizontal force was applied monotonically and the opening and slip displacements were recorded. For D type specimens, the opening and slip displacements were controlled so that the specimen experienced the same displacement path with the companion C type specimen. In this manner, the shear resistance by the dowel action was measured by D type specimens and the shear resistance by the concrete action was computed by subtracting shear force of a D type specimen from the shear force of a companion C type specimen. Opening and slip displacements were measured at four corners of the specimen. Two strain gages were placed on the surface of dowel bars 25 mm above the interface so that the bending and axial components of deformation was computed.

TEST RESULTS

Shear Stress –Slip Relations

Figure 4 shows shear stress- slip relations for five representative specimens, all of which had concrete strength of 50 MPa. For C type specimens, shear stress first increased without noticeable slip and then dropped suddenly with large slip. This drop was larger for specimens with lower ρf_y, where ρ is the area ratio of dowel bars to the construction joint and f_y is the yield strength of dowel bars. The shear stress then increased gradually with slip and the initial peak was exceeded for specimens with higher ρf_y. It is considered that the initial peak emerged due to the cohesion at the concrete interface. After a distinctive interface was formed, the shear resistance was provided by the concrete and dowel actions. Shear stress for D type specimens increased monotonically with increasing slip. Setting τ_D as the stress transferred in a D type specimen and τ_C as that in a companion C type specimen, the contribution of the dowel action to the total shear is expressed as τ_D/τ_C. The computed results from six sets of Series 1 specimens are shown in Fig. 5. Up to slip equalled 4 mm, τ_D/τ_C increased gradually from 0 to about 60%. Comparing L10-30 with H10-30, L10-50 with H10-50, and L10-80 with H10-80, τ_D/τ_C for higher ρf_y is larger than that for lower ρf_y. However, comparing specimens with a same ρf_y value, it can be seen that concrete strength did not have clear influence on τ_D/τ_C.

Some design practices do not allow any slip at construction joints but studies [8] show that the structure with interface slip less than 2 mm performs as good as that with rigid interfaces. Figures 4 and 5 show that slip does not necessarily cause a brittle failure and even the increase in shear capacity can be expected for larger ρf_y. The interface endures large slip without much degradation in shear capacity since the dowel action becomes dominant after slip greater than 2 mm. For these reasons, the shear capacity was defined for C type specimens as the maximum shear stress for slip under 2mm and these values are listed in Table 1.

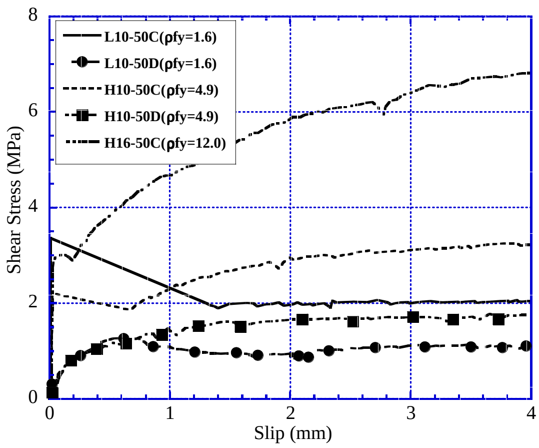

Figure 4: Shear stress – slip relations

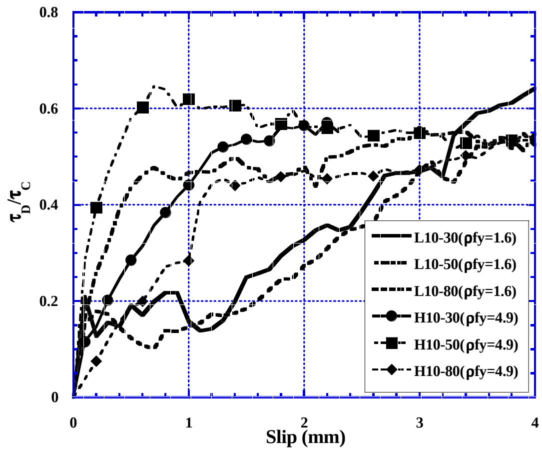

Figure 5: τ_D/τ_C– slip relations

Surface Roughness

The surface roughness of joints was quantitatively evaluated to study its correlation with the shear capacity, the stiffness in shear-slip relation, and the slip-opening relation. In this study, the existing four indices were employed to express the roughness; the fractal dimension, D, the root mean square height, H_{rms}, the average height, H_{ave}, and the core roughness depth, R_k. The details for these indices are not explained here and readers are suggested to read references 5, 6, and 10 for details. To obtain D, a rectangle of 10 mm by 20 mm were divided into a 32 by 32 grid and the height was measured at each grid point using a three dimensional laser digitizer. One value of D was computed from each rectange and 27 rectangles were used to obtain the average. Values H_{rms}, H_{ave}, and R_k were computed from 1000 measured heights along a 100 mm long straight base line. Assuming the obtained data is expressed as $y = f(x)$ as shown in Fig. 6, H_{rms} and H_{ave} is expressed as Eqs. 1 and 2, respectively. R_k was evaluated from the linear representation of the material ratio curve (also referred to as the Abbott curve) which describe the increase of the material portion of the surface with increasing depth of the roughness profile. One value of H_{rms}, H_{ave}, and R_k was obtained from a measurement along one base line and nine base lines were used to obtain the average. In Table 3, the roughness of specimens in Series 2 are expressed using four indices. All indices have large standard deviation and a same kind of finishing with different concrete strengths (e.g. H50P and H100P) did not necessarily have similar indices. The correlations between one of these four indices and either of the shear capacity, the stiffness in shear-slip relation, or the slip-opening relation were studied but none of those combinations showed the clear correlation. For example, Fig. 7 shows the shear capacity – R_k relations and the correlation is not very clear. Since quantitative evaluation of the roughness is one of the important tasks for the interface shear transfer, an effort to find a more appropriate index is under way.

$$H_{rms} = \sqrt{\frac{1}{L}\int_0^L \left(f(x)\right)^2 dx} \qquad (1)$$

$$H_{ave} = \frac{1}{L}\int_0^L |f(x)| dx \qquad (2)$$

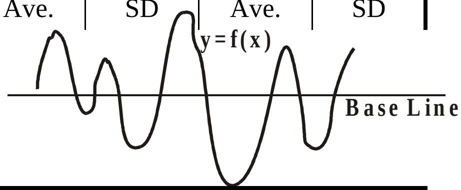

Figure 6: Surface roughness

Table 3: Indices for surface roughness

	D		H_{rms} (mm)		H_{ave} (mm)		R_k (mm)	
	Ave.	SD	Ave.	SD	Ave.	SD	Ave.	SD
H50N	2.003	0.001	0.09	0.05	0.07	0.04	0.16	0.10
H50P	2.271	0.202	1.39	0.38	0.99	0.27	2.46	1.10
H50R	2.019	0.009	0.80	0.23	0.59	0.15	1.42	0.36
H50T	2.032	0.015	1.66	0.24	1.40	0.21	3.76	1.00
H100N	2.003	0.001	0.14	0.04	0.12	0.04	0.33	0.10
H100P	2.234	0.222	1.84	0.66	1.42	0.56	3.60	1.39
H100R	2.050	0.049	1.06	0.36	0.81	0.25	2.26	0.64
H100T	2.031	0.018	2.34	0.14	2.00	0.12	6.50	0.77

Ave.: Average SD: Standard deviation

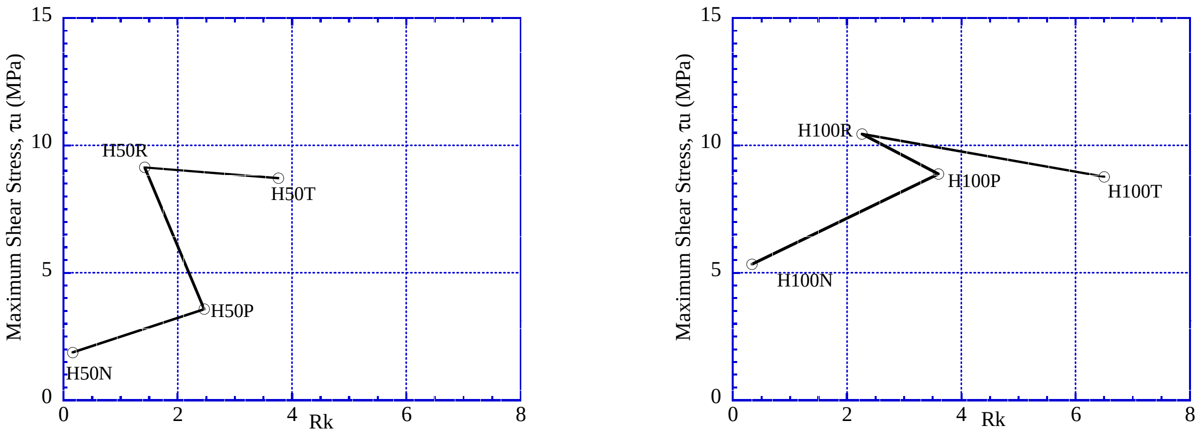

(a) f'c = 50 MPa (b) f'c = 100 MPa

Figure 7: Shear capacity – R_k relations

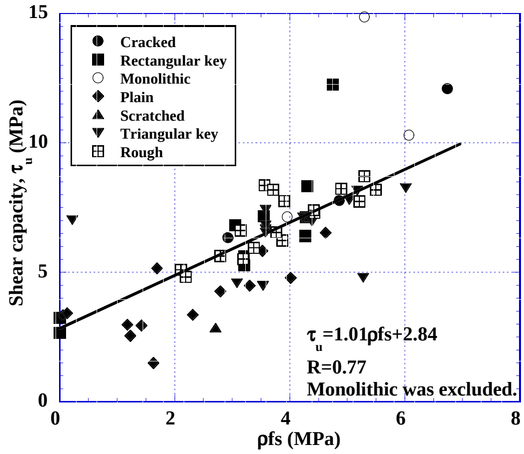

Figure 8: Shear capacity -ρf_s relations

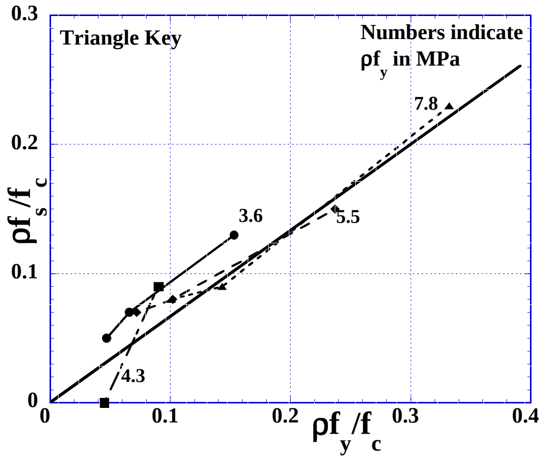

(a) Triangle shear key

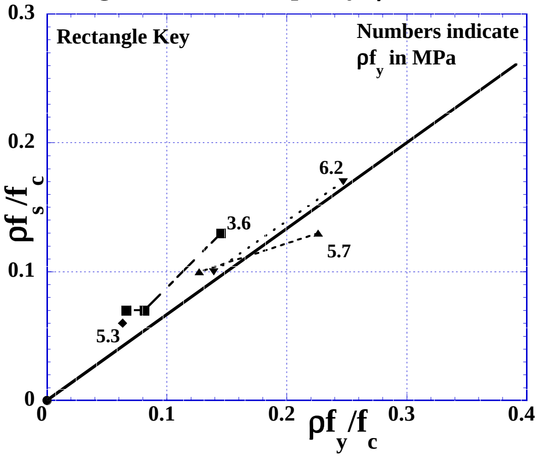

(b) Rectangle shear key

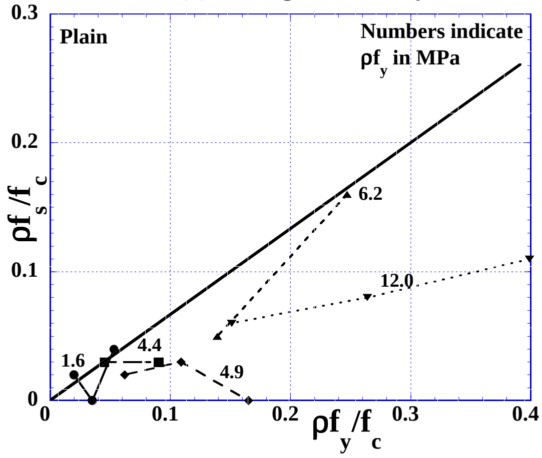

(c) Plain surface

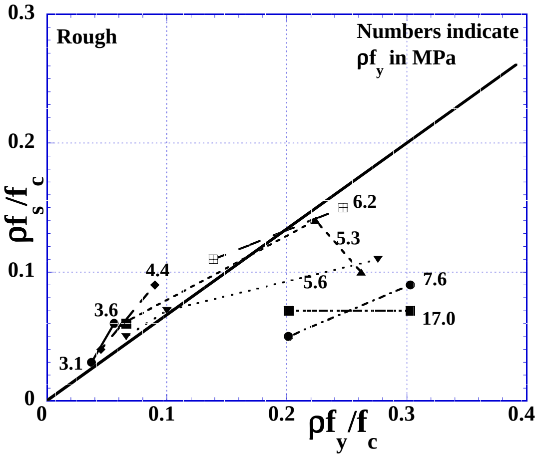

(d) Rough finishing

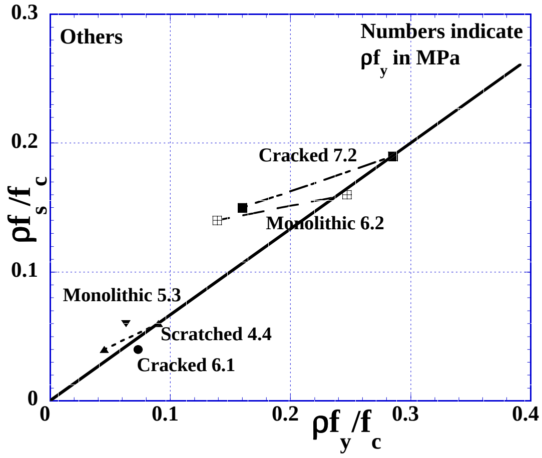

(e) Others

Figure 9: $\rho f_s/f'_c$ – $\rho f_y/f'_c$ relations

Shear Capacity

Although shear capacity should not be the only design criteria to check the performance of joints, it is still a important design factor. The current design for interface shear is based on Mattock and Hawkins' research [7] and expressed by Eq. 3.

$$\tau_u = 0.8\rho f_y + 1.4 \le 0.3 f'c \qquad \text{(MPa)} \qquad (3)$$

where ρ is the area ratio of dowel bars to the joint, f_y the yield strength of dowel bars, and f'_c the compressive strength of concrete. In the experiment, dowel bars did not generally yield when the maximum shear was reached as shown in Table 1. So it was concluded that the shear capacity should be correlated to the normal stress ρf_s where f_s is the tensile stress of dowel bars at the maximum shear. Figure 8 shows the relation between τ_u and ρf_s from the test results of this study and reference 9. Concrete strength ranged from 20 MPa to 98 MPa, yield strength of dowel bars from 309 MPa to 1334 MPa, dowel bar ratio from 0.4 to 1.95, area of constuction joint from 160 cm^2 to 576 cm^2, and a diameter of dowel bars from 10 mm to 16 mm. Surface conditions were plain, triangle, rectangle key, monolithic and precracked. All experiments were under monolithic loading. Excluding three monolithic specimens shown in white circle, the relations between τ_u and ρf_s can be expressed by Eq. 4 from a regression analysis.

$$\tau_u = 1.01\rho f_s + 2.84 = 1.01 \times \frac{\text{Normal force}}{\text{Joint area}} + \text{Cohesion} \quad \text{(MPa)} \qquad (4)$$

The correlation coefficient was 0.77. In Eq. (4), τ_u is expressed by a summation of the frictional term and the cohesion term as Eq. 3. Here, f_s is unknown in order to predict τ_u and this value should be computed from known values in order to design joints. To predict f_s, the relation between $\rho f_s / f'_c$ and $\rho f_y / f'_c$ was studied as shown in Fig. 9. Nonlinear relations which are dependent on a surface finishing seem to exist between $\rho f_s / f'_c$ and $\rho f_y / f'_c$. However, the number of specimens for each surface finishing was not enough to deduce the mathematical relation between $\rho f_s / f'_c$ and $\rho f_y / f'_c$. Expressing the roughness quantitatively was also difficult as explained in Section 3.2. For these reasons, a simple linear curve was used to express $\rho f_s / f'_c$ - $\rho f_y / f'_c$ relation.

$$\rho f_s / f'_c = 2/3 \cdot \rho f_y / f'_c \qquad (5)$$

that is,

$$f_s = 2/3\, f_y \qquad (6)$$

Equation 6 is shown in thick solid straight lines in Fig. 9. The equation does not represent the behavior for plain surface and ρf_y more than 7.6 MPa for rough finishing. Substituting Eq. (6) in Eq. (3), the maximum shear strength can be predicted as Eq. (7).

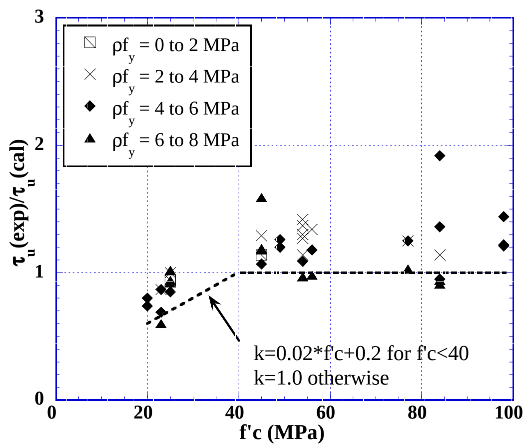

Figure 10: τ_u/τ_{cal} – f'_c relations

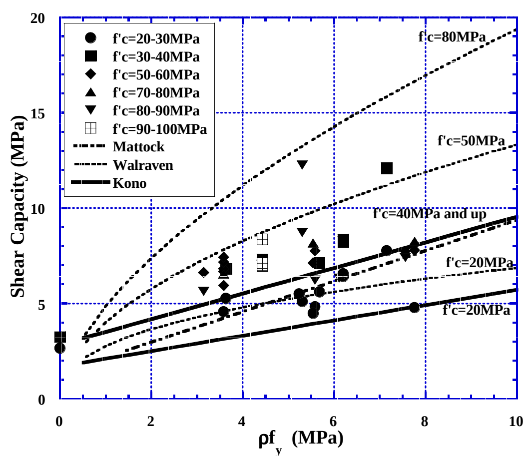

Figure 11: Shear capacity - ρf_y relations

$$\tau_u = 0.67\rho f_y + 2.84 \qquad \text{(MPa)} \qquad (7)$$

Prediction using Equation (7) is shown in Fig. 10. It may be seen that the prediction for the concrete strength less than 40 MPa is uncerservative. So the reduction factor k shown in dotted line was multiplied to Equation (7).

$$\tau_u = k(0.67\rho f_y + 2.84) \qquad \text{(MPa)} \qquad (8)$$

where $k = 0.02 f'c + 0.2$ for $f'c \le 40$ MPa and $k = 1.0$ otherwise.

Not applicable to plain surface and ρf_y more than 7.6 MPa.

Prediction by Eq. 8 is shown with thick solid lines in Fig. 11 and compared with Eq. 3 and Walraven's equation [11]. The proposed equation is similar to Eq. 3 and is less influenced by the concrete strength. The test results also shows similar variations.

CONCLUSIONS

1. The increase in the contribution of dowel bars to the total shear was larger for high ρf_y although the contribution eventually reached about 60% at slip of 4 mm no matter what ρf_y was. The concrete strength did not have much influence on the contribution of the dowel action. With larger amount of ρf_y, the stress drop from the initial peak decreased and the stress regain after the drop increased.
2. The shear capacity was considered to be a linear function of the normal force exerted by dowel bars but the design should take into account the fact that dowel bars did not yield when the shear capacity was reached. This normal force can be predicted using $\rho f_s / f'_c$ and $\rho f_y / f'_c$ relations which is nonlinear and dependent on the roughness of the interface.
3. For a design purpose, the relation between $\rho f_s / f'_c$ and $\rho f_y / f'_c$ was approximated by a linear curve and the shear capacity was expressed with an equation similar to that by Mattock and Hawkins.
4. Four indices were used to express surface roughness but none of them clearly differentiated different surface finishings prepared in this study or showed close relation to stiffness and capacity in shear.

AKNOWLEDGEMENT

This research was financially supported by Prestressed Concrete Cooperative Research and the Japan Educational Ministry (Grant Number 10750430).

REFERENCES

1. ACI Committee 318 (1991), *Building Code Requirements for Reinforced Concrete*, American Concrete Institute, Detroit, MI.
2. Ali, M. A. and White, R.N. (1999), "Enhanced Contact Model for Shear Friction of Normal and High-Strength Concrete," *ACI Structural Journal, V. 96, No. 3, May-June,* pp. 348-360.
3. Architecture Inst. of Japan (1982), 'Standard for Structural Calculation of Prefabricated RC Structures with Shear-Walls.'
4. Dulacska, H. (1972), "Dowel Action of Reinforcement Crossing Cracks in Concrete," *ACI Journal, Dec.*, pp. 754-757.
5. ISO/DIS 13565-2 (1994), 'Characterization of Surface Having Stratified Functional Properties, Part 2: Height Characterization of Using the Linear Material Ratio Curve,' *International Organization for Standardization*.
6. Katori, K., Hayashi, S., Makitani, T, and Ushigaki, K. (1998), 'Estimate of the shear strength of construction joint by using its surface roughness and characteristic of slip displacement of joint under shear force,' *J. of Struct. and Constr. Eng.*, Architecture Inst. of Japan, No. 507, May, pp. 107-116.
7. Mattock, A.H. and Hawkins, N.M. (1972), "Shear Transfer in RC Recent Research," *PCI Journal, March-April*, pp. 55-75.
8. Obuchi, H. et al. (1997), 'Study on shear transfer considering shear displacement in connenction of precast concrete,' *J. of Struct. and Constr. Eng.*, Architecture Inst. of Japan, No. 491, Jan., pp. 97-104.
9. Okamoto, H. et al. (1990-1992), "Shear Transfer between High Strength Precast and Cast-in-situ Concrete," *Summaries of Technical Papers of Annual Meeting, Architecture Institute of Japan*, pp. 539-540(1990) pp. 679-680(1991) pp. 773-774(1992).
10. Underwood, E. E. and Banerji, K. (1986), 'Fractals in Fractography,' *Material Science Engineering*, Vol. 80, pp. 1-14.
11. Walraven, J., Frenay, J., and Pruijssers, A. (1987), "Influence of Concrete Strength and Load History on the Shear Friction Capacity of Concrete Members," *PCI Journal, Jan.-Feb.*, pp. 66-84.